International Journal of Applied Electromagnetics in Materials 3 (1992) 73–85
Elsevier

Simulated levitation characteristics of magnetic suspension system by linear induction motor

Takashi Hikihara and Yoshihisa Hirane
Department of Electrical Engineering, Kansai University, Yamate-cho 3-3-35, Suita, Osaka 564, Japan

Received 1 May 1991

In this paper, a model for simulation of a developed magnetic suspension system by a linear induction motor is induced. The system has a linear induction motor (LIM) as a primary guide way, and a U-shaped iron core, on which the secondary winding is wound, is set at the center top of the vehicle. The vehicle has no electrical contact with the guide way and the configuration of the system is very simple. In the experimental system, however, it is difficult to decide the parameters. Therefore, the model plays an important role to confirm the stability of the suspended motion and to obtain a stable parameter region. Through several analyses, it is proved that the vehicle can be levitated by the proposed control method. Moreover, it is also cleared that chaotic motions occur at some parameter area in the domain of levitation.

1. Introduction

In semiconductor factories it is well known that dust causes a decrease in the yield rate. The factory automation system, which is used in a clean-room, needs to be completely dustless. The conveyance systems applied in the factory automation system have so many dust sources that many kinds of magnetic levitation systems are proposed as an alternative system.

We have developed a magnetic suspension system by the linear induction motor (LIM) [1–3]. The system has a linear induction motor to suspend and to carry a vehicle. In order to obtain the suspending and driving forces, a U-shaped iron core with secondary winding is fixed at the center top of the vehicle. Generally speaking, the attraction type magnetic suspension system without any feedback control is essentially unstable. The proposed system adopts the method that the forces are controlled by the short-circuit and open-circuit of the secondary winding using a transistor switch. The developed system uses the magnetic field of LIM both to suspend and to carry the vehicle. However, in this paper the levitation characteristics are mainly discussed.

In order to obtain stable levitation characteristics, the transistor is switched with reference to a function of the gap displacement and the velocity of displacement. The levitation characteristics have been discussed experimentally. In this paper, a model for the simulation of the developed magnetic suspension system is induced to confirm the dynamical mechanism of levitation and to decide the parameters. Moreover, the levitation characteristics are discussed numerically. Through the analyses, it is also made clear that chaotic motions occur at some parameter area in the domain of levitation.

Correspondence to: Dr. T. Hikihara, Department of Electrical Engineering, Kansai University, Yamate-cho 3-3-35, Suita, Osaka 564, Japan.

2. System configuration of magnetic suspension system

2.1. Principles of magnetic suspension

Attraction type magnetic suspension systems are essentially unstable without any control of the suspending force. The schematic system configuration is shown in fig. 1. The upper U-shaped core means an equivalent magnetic circuit of LIM and the lower one the fixed U-shaped core on a vehicle. To obtain the attracting magnetic force, the LIM is fed by an AC voltage V_1. When the position of the vehicle is lower than the directed position as shown in fig. 1a, the switching transistor S_1 is turned off. Then the vehicle is attracted toward LIM. When the position of the vehicle is higher than the directed position as shown in fig. 1b, the switching transistor is turned on. Then the vehicle is repulsed against the LIM by the magnetic force caused by the current in the secondary winding. Changing the transistor (on–off) mode between the attractive and the repulsive state, the vehicle can be held near a directed position.

2.2. System configuration

The system configuration is shown in fig. 2. A LIM is arranged at the upper side as a primary guide way and a U-shaped core is fixed at the center top of the vehicle, which is given by a horizontal board in fig. 2. To control the magnetic attracting force, the secondary winding is equipped on the core. The winding is connected with a diode bridge circuit and the current is changed into a direct current. The DC terminal of the bridge circuit parallels both a transistor and a resistor. The resistor has a role to protect the transistor from switching surge. The resistor is equivalent to an internal resistance of the

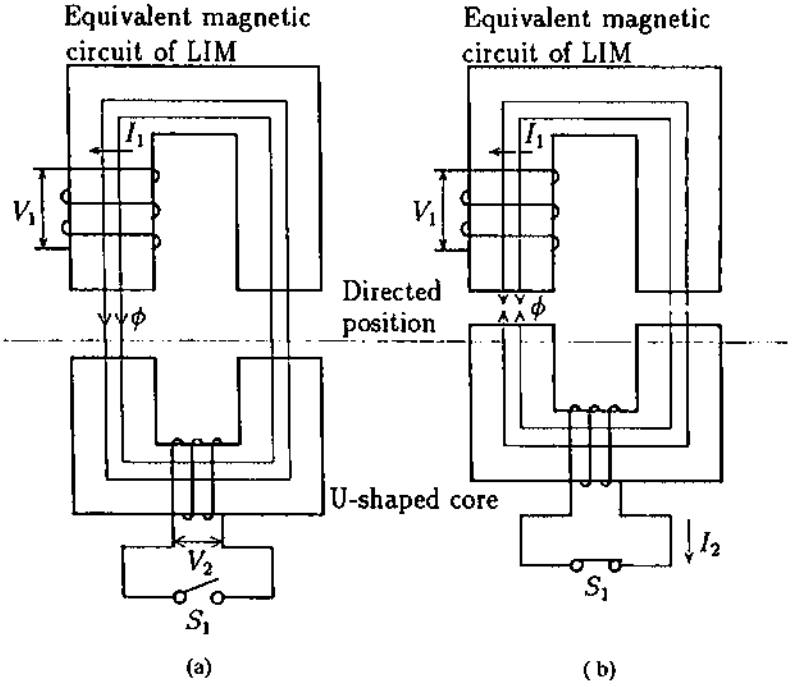

Fig. 1. Principles of suspension control of the system: (a) the attracted state (S_1: off), (b) the repulsed state (S_1: on).

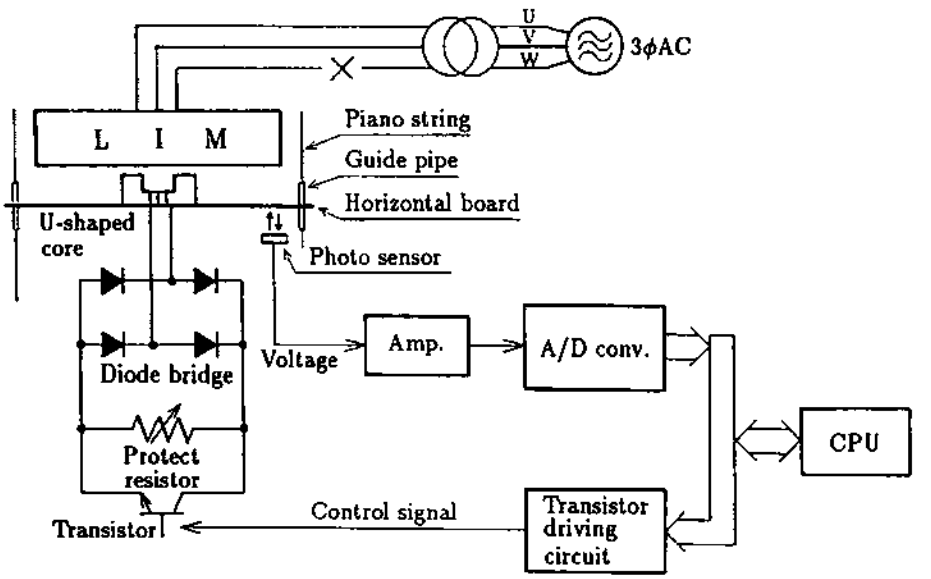

Fig. 2. System configuration.

charging circuit of a battery in the planned prototype system. By switching the transistor, the resistance of the secondary circuit can be changed discretely.

To examine the stability of levitation, it is not necessary to generate the driving magnetic force by LIM. The LIM is fed only by a u,v-phase voltage as a single phase excited state. Moreover, the freedom of the vehicle is limited to the up and down direction by vertically stretched piano strings and guide pipes at the corners of the horizontal board.

2.3. *Control method*

The principal method for suspension control is given in section 2.1. However, it is difficult to stabilize the levitated motion of a vehicle only by the application of the method. Then, the experimental system adopts the method which decides the timing of switching by reference to the following function S of the gap displacement x and the velocity of the displacement y:

$$y = -a(x - x_0)\,, \tag{1}$$

where x_0 denotes a directed position and a is the slope of the switching line on the phase plane. Here, the positive directions of x and y are defined as the directions opposite to LIM. The switching function S on the phase plane (x, y) is shown in fig. 3. In the upper (right) side of the line the transistor is turned off. On the other hand, the transistor is turned on in the lower (left) side. The timing of switching is given at the instant when the trajectory of the vehicle motion intersects the line S on the phase plane transversally. As a result, the vehicle can be brought near the directed position smoothly. This type of control can be called bang-bang control or VSS [4].

However, fig. 3 shows a typical phase portrait obtained by the DC magnetic force. The phase portrait driven by the AC magnetic force is periodically changed. Therefore, sampled points of the trajectory at the frequency of excited LIM current follow the phase portrait in fig. 3. That is, the suspended motion can be finally brought to a periodic levitated motion by means of the control method which uses the switching function on the two-dimensional phase plane.

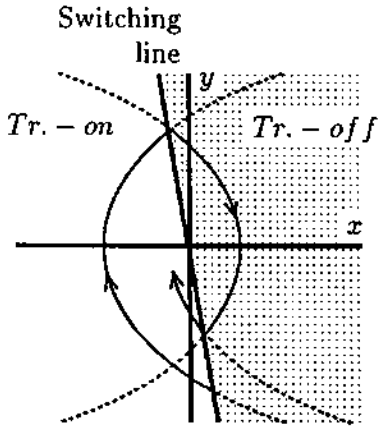

Fig. 3. Concepts of the switching control method.

2.4. Dynamical system model

2.4.1. Kinetic equation

The developed magnetic suspension system has many parameters which can be arranged initially. Table 1 denotes their definitions. As the freedom of the vehicle motion is limited only to the up and down direction, all forces which operate upon the vehicle are shown in fig. 4. The downward forces consist of the gravitation Mg and the repulsive force F_2 caused by the current of secondary winding. On the other hand, the upward forces consist of the attracting force F_1 caused by the LIM current and the damping force $k\,\mathrm{d}x/\mathrm{d}t$. The kinetic equation is given by

$$M\frac{\mathrm{d}^2x}{\mathrm{d}t^2} + k\frac{\mathrm{d}x}{\mathrm{d}t} - Mg + F_1 - F_2 = 0\,. \tag{2}$$

The attracting force F_1 and the repulsive force F_2 are generated by the magnetic flux ϕ through the LIM and the U-shaped iron core. The magnetic flux ϕ is given by magnetic circuit theory as follows:

Table 1
System parameters and variables

Symbol	parameter/variable
g	Acceleration of gravity
M	Mass of vehicle
k	Damping coefficient
μ_m	Magnetic permeability of air-gap
S_c	Cross section of U-shaped core
N_1	Number of turns of LIM winding
N_2	Number of turns of secondary winding
i_1	Excited current of LIM winding
i_2	Current of secondary winding
I_1	Amplitude of excited LIM current
ω	120π
L_2	Inductance of secondary winding
R	Protection resistor
r_e	Conduction resistance of transistor

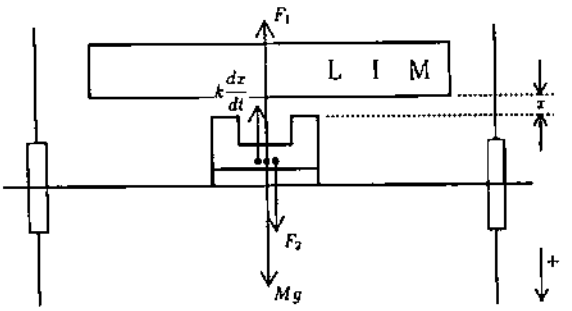

Fig. 4. Forces which operate on the vehicle.

$$\phi = \frac{\mu_0 S_c}{2x} (N_1 i_1 - N_2 i_2) , \tag{3}$$

where i_1 denotes the LIM current and i_2 the current of secondary winding. Then, the gross of the magnetic attracting force and the repulsive force, $-F_1 + F_2$, is given by

$$-F_1 + F_2 = -\phi^2 / \mu_0 S_c . \tag{4}$$

Eqs. (2)–(4) describe the kinetic relations of motion.

2.4.2. Circuit relations of secondary winding

The exciting current of LIM, i_1, always keeps a constant amplitude, because the windings on the LIM poles, which do not oppose the U-shaped core of the vehicle, operate as leakage inductances. The current is given by

$$i_1 = I_1 \sin \omega t , \qquad \omega = 120\pi . \tag{5}$$

The current of the secondary winding, i_2, continuously changes, in spite of the discrete turn of the transistor on–off mode. In the case of the on-mode, the resistance of the secondary winding consists of the conduction resistance r_e of the transistor and the protection resistor R. They are parallel connected. In the case of the off-mode, the resistance of the transistor becomes an infinite value. When the voltage drop of the switched resistance is given by $f(i_2)$, the circuit equation is as follows:

$$N_2 \frac{\mathrm{d}\phi}{\mathrm{d}t} = L_2 \frac{\mathrm{d}i_2}{\mathrm{d}t} + f(i_2) , \tag{6}$$

where

$$f(i_2) = \begin{cases} R r_e i_2 / (R + r_e) & \text{(Tr: on)} , \\ R i_2 & \text{(Tr: off)} . \end{cases}$$

2.4.3. System equations

Based on the above consideration, the levitation characteristic of the system is given by the following simultaneous ordinary differential equations:

$$\frac{\mathrm{d}x}{\mathrm{d}t} = y ,$$

$$\frac{\mathrm{d}y}{\mathrm{d}t} = g - \frac{\mu_0 S_c}{4M} \frac{(N_1 i_1 - N_2 i_2)^2}{x^2} - \frac{k}{M} y ,$$

$$\frac{\mathrm{d}i_1}{\mathrm{d}t} = I_1\omega\cos\omega t\,, \tag{7}$$

$$\frac{\mathrm{d}i_2}{\mathrm{d}t} = \left(1+\frac{\mu_0 S_c N_2^2\gamma}{2L_2 x}\right)^{-1}\left(-\frac{\mu_0 S_c N_2}{2L_2}\,\frac{y}{x^2}\,(N_1 i_1 - N_2 i_2) + \frac{\mu_0 S_c N_1 N_2}{2L_2}\,\frac{1}{x}\,\frac{\mathrm{d}i_1}{\mathrm{d}t} - \frac{1}{L_2}\,f(i_2)\right).$$

Here, a coefficient γ,which corresponds to the effect by leakage flux of the secondary winding according to the change of gap displacement, is introduced.

By the transformation, $N_1 i_1 \to i_1$, and $N_2 i_2 \to i_2$, the following simplified equations are obtained:

$$\begin{aligned}
\frac{\mathrm{d}x}{\mathrm{d}t} &= y\,,\\
\frac{\mathrm{d}y}{\mathrm{d}t} &= a_1 + \frac{a_2(i_1-i_2)^2}{x^2} - a_3 y\,,\\
\frac{\mathrm{d}i_1}{\mathrm{d}t} &= a_4\cos\omega t\,,\\
\frac{\mathrm{d}i_2}{\mathrm{d}t} &= \frac{x}{x+a_5}\left(-a_6\,\frac{y(i_1-i_2)}{x^2} + a_6\,\frac{1}{x}\,\frac{\mathrm{d}i_1}{\mathrm{d}t} - a_7 f(i_2)\right),
\end{aligned} \tag{8}$$

where

$$\begin{aligned}
&a_1 = g = 9.8\,, \quad && a_2 = \mu_0 S_c/4M\,, && a_3 = k/M\,,\\
&a_4 = N_1 I_1\omega\,, && a_5 = \mu_0 S_c N_2^2\gamma/2L_2\,, && a_6 = \mu_0 S_c N_2^2/2L_2\,,\\
&a_7 = 1/L_2\,.
\end{aligned} \tag{9}$$

These equations are not normalized, because of the easy comparison with experimental results. In these inductions, the following assumptions are used:

(1) The conduction resistance of the diode bridge and the resistance of the secondary windings are negligible.
(2) The leakage flux of LIM can be neglected.
(3) The inductance of the secondary winding, which will depend upon the gap displacement, stays almost constant. Also, the change of reluctance can be neglected.
(4) The mechanical resonance and the distortion of the horizontal board can be neglected.

In spite of these assumptions, eq. (8) is considered to hold the fundamental characteristics of the system.

3. Results of numerical analysis

In this section, the numerical results of eq. (8) are discussed in several cases. The system which is represented by eq. (8) must be described in three-dimensional space (x, y, i_2). In this paper, only the levitation characteristics are discussed and the driving characteristic are not taken into account. Therefore, the system is easily grasped by the projection onto the two-dimensional system (x, y), in which the secondary current does not appear explicitly.

3.1. Domain of levitation

By making use of the switching control on the phase plane, the domain of levitation can be obtained. Figure 5 shows the calculated results of the domain, which is obtained on the protection resistor R – the

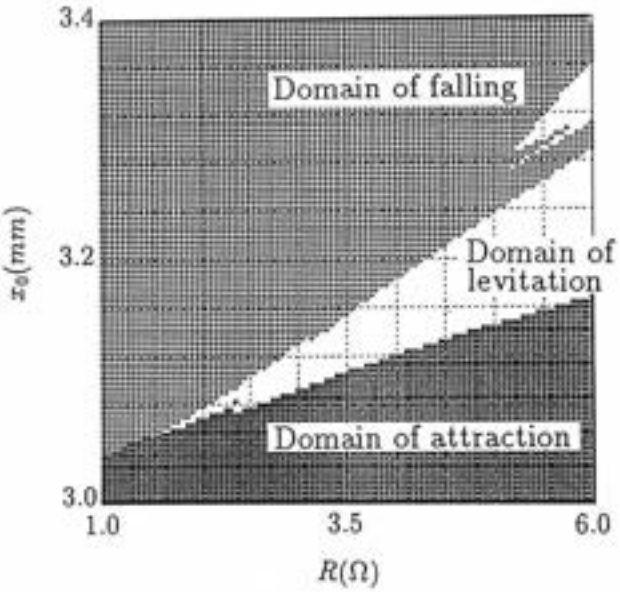

Fig. 5. Domain of levitation.

directed position x_0 plane. In the figure, the domain of attraction toward LIM (the deep hatched area), the domain of levitation (the white area), and the domain of falling (the thin hatched area) are shown. Figure 5 corresponds to the cases in which the gradient a of eq. (1) is fixed at 400. In the analysis, the amplitude of the LIM current I_1 is set at 6.0 A, the damping coefficient k at 80, the leakage coefficient γ at 2, and the mass of the vehicle M at 780 g. They correspond to the value of our experimental system. The initial position on the phase plane is at $(x, y, i_2) = (x_0, 0, 0)$. In the following discussions a is always kept at 400.

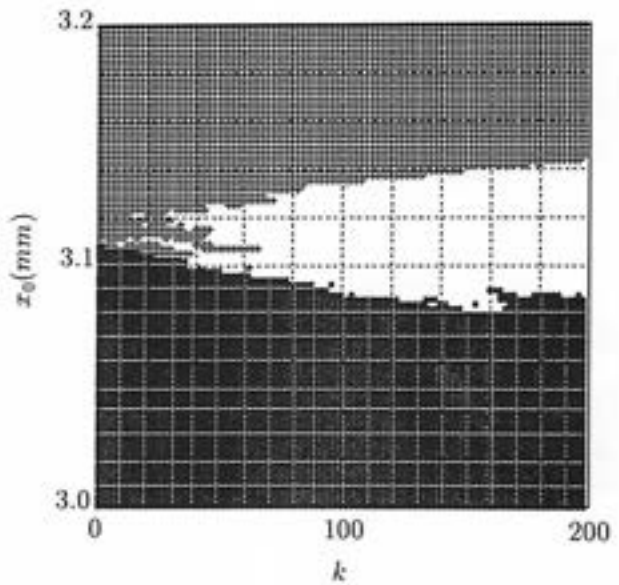

Fig. 6. Damping coefficient dependence of the levitation domain.

3.2. Damping characteristics and mass dependence

In the former section, we chose the damping coefficient $k = 80$. Figure 6 shows a domain of levitation on the damping coefficient k – the directed position x_0 plane. In the calculation, the protection resistor R is fixed at 3.0 Ω and the other parameters are the same as in the case of fig. 5. According to the increase of the damping coefficient, the domain of levitation is likely to become wide. On the basis of comparison of the trajectories in the numerical analysis with those in the experiments, the damping coefficient k can be obtained as 80.

Figure 7 shows a domain of levitation on the mass M – the directed position x_0 plane. The horizontal axis means the increased mass of the vehicle. The protection resistor is fixed at $R = 3.0\,\Omega$ and the other parameters are the same as in the case of fig. 5. There can necessarily be found a domain of levitation in the region where M is less than 0.2 kg. According to the increase in mass, the directed position must be closed to LIM.

3.3. Levitation characteristics

After the long time continuous calculation of the suspended motion, the transient state converges to three states. The levitated state of the vehicle exists between the attracting area to LIM and the falling area.

Figure 8 shows the boundary of the domains in fig. 5. We chose typical parameter points from a to n in the domain. The phase plane trajectories at the points are shown in fig. 9. The solid line in the figures is the switching line. The domain of levitation is separated into two areas, which are denoted area I and II in fig. 8. Near the domain of attraction in area I, the trajectories are likely to be irregular. On the other hand, the trajectories are periodic near the domain of falling in area I. It becomes a single shaped trajectory from the double shaped one according to being far from the LIM. In area II, the trajectory is always single shaped.

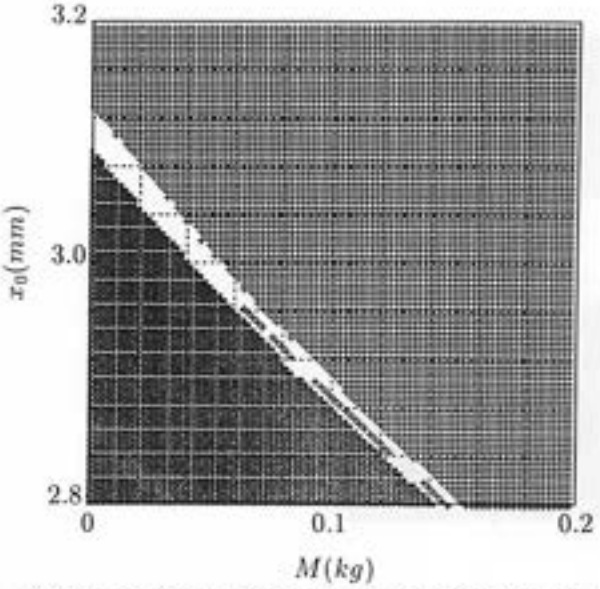

Fig. 7. Increased mass dependence of the levitation domain.

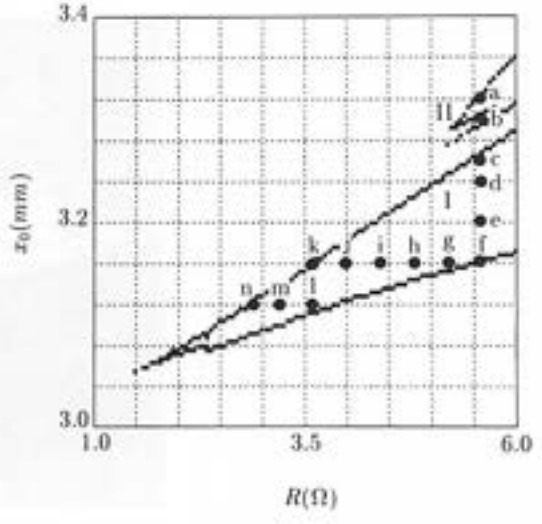

Fig. 8. Boundary of levitation domain and calculated parameters.

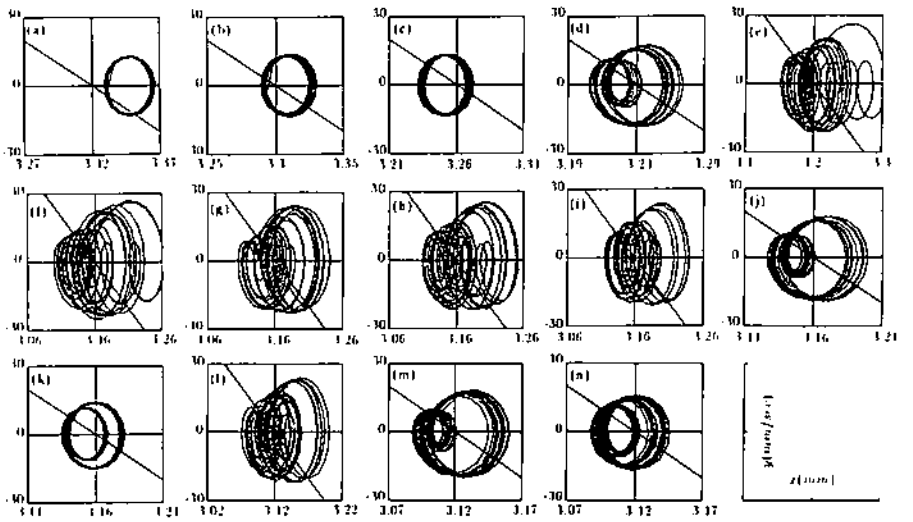

Fig. 9. Phase plane trajectories.

Figure 10 shows the gap displacement, the velocity of the displacement, the transistor mode and the spectrum ratio at the typical parameter points (b), (e), and (k). Figure 11 shows the Poincaré map of the trajectory at (e). The Poincaré map experimentally means the plot of sampled points of a trajectory on the phase plane by the frequency which synchronizes to the exciting force of the system. In the analysis, the frequency is fixed at 60 Hz, which is the frequency of the exciting LIM current. When the trajectory shows the periodical steady state like (a), the map gathers a point. However, when the motion of the vehicle is irregular, the map distributes widely. In the field of nonlinear dynamics, the irregular motions, which is called "chaos", can be found [5–7]. Our system also has the irregular

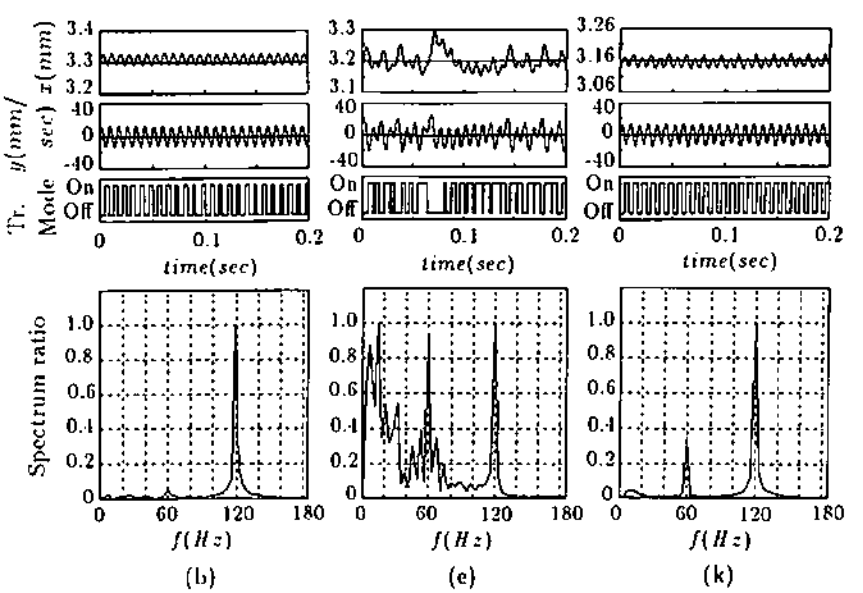

Fig. 10. Gap displacement, velocity of displacement, switching patterns, and spectrum of vibration of the gap displacement.

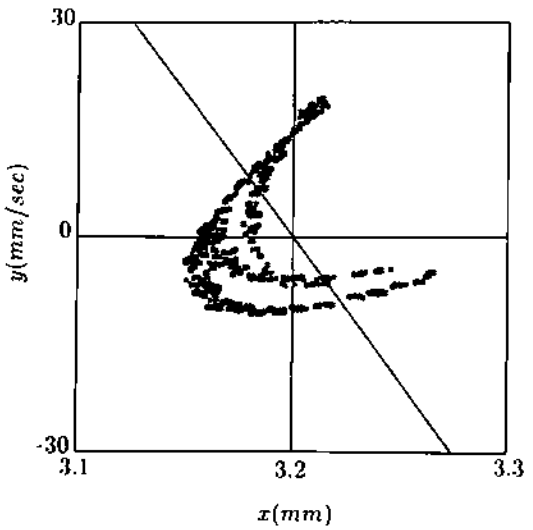

Fig. 11. Poincaré map of trajectory at (e).

motions in the domain of levitation. Based on figs. 9, 10, and 11 the motions are considered to be chaotic. In sight of the levitation control, the mechanism of chaotic motion must be grasped clearly. Moreover, in this three-dimensional non-autonomous system, the relations between the chaotic motions and VSS control have to be researched in detail.

3.4. *Trajectory bifurcation*

By means of the points at which the trajectory crosses the switching line from the left side to the right side transversally, a one-dimensional mapping can be defined [8]. Figure 12 shows the bifurcation

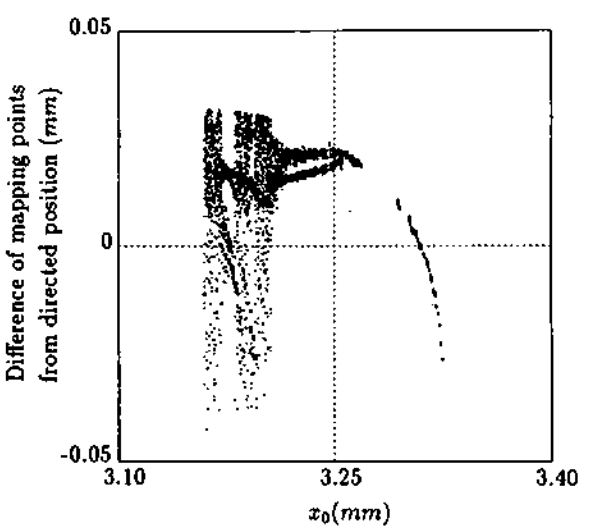

Fig. 12. Bifurcation diagram.

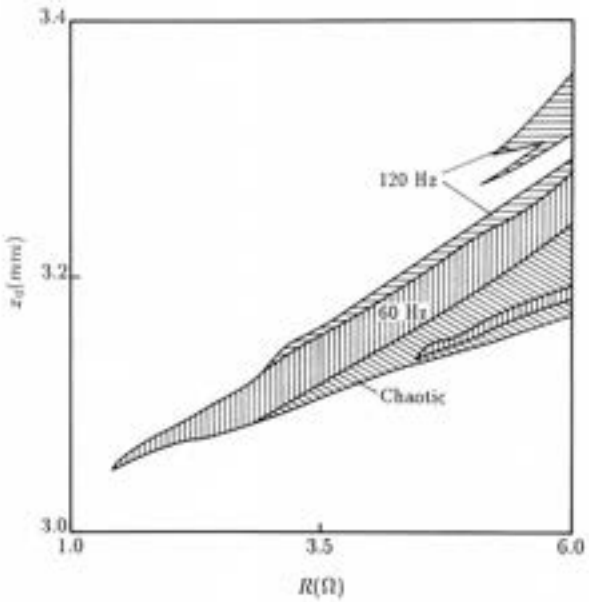

Fig. 13. Classification of the levitation domain.

diagram of the points according to the upward shift of the directed position x_0 with keeping $R = 5.6\,\Omega$. The change of trajectory, which is shown in fig. 9, can be explained as "pitch-fork bifurcation". Based on the bifurcation, the domain of levitation can be classified as shown in fig. 13. The periodical trajectories are found in the area near the domain of falling. As the directed position x_0 closes to LIM, the trajectories bifurcate and chaotic motions appear at $R > 3\,\Omega$.

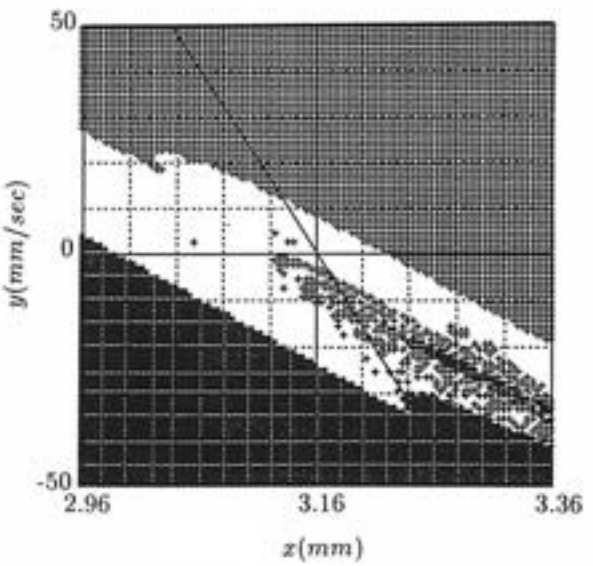

Fig. 14. Initial value dependence of the levitation domain.

3.5. Initial value dependence

The former results are obtained by calculation from an initial directed position on the phase plane (x, y) with the velocity of displacement y and the secondary current i_2 at 0. Here, we examine whether the levitation characteristics depend upon the initial position and velocity, or not. Figure 14 shows the initial value dependence which is obtained by the scanning on the phase plane (x, y) at (k) in fig. 8. At the beginning of calculation, i_2 is also fixed at 0. Each hatched area corresponds to the domains in fig. 5, respectively. The domains of attraction to LIM and the falling enter into the domain of levitation complicatedly. It is shown that the directed position with no velocity is not necessarily appropriate to the initial value for levitation. Besides the parameter region I and II in fig. 8, there cannot be found any levitation area in the initial position and velocity plane.

4. Conclusion

In this paper, a model for the analysis of magnetic suspension system by a linear induction motor is induced. By making use of the model, the detailed levitation characteristics are examined numerically. As a result of the analyses, it is clarified that the adopted control method has an effect to hold the vehicle near a directed position. In the case of a non-autonomous system, like the proposed system, the periodical states are considered to be stable states. However, even when the vehicle is levitated, the motion is not necessarily periodic, because it is also clarified that a kind of chaotic motion can be found in the system.

These results are considered to be conservative. The experimental system has a larger domain of levitation and is robust. The reason is that the model for simulation has some assumptions. Especially, the reluctance force may have an effect on the stability in the case of wide gap. In this paper, we have treated a periodical steady state with the small amplitude. Therefore, the results in this paper are the ascertainment in principle.

VSS, which is adopted to the proposed magnetic suspension system, is well known as one of the effective control methods to nonlinear systems. However, the VSS control method is usually applied to an autonomous dynamical system. Therefore, in the case of our proposed non-autonomous system, the stability must be ensured theoretically. The obtained results show that the system can be stabilized by the VSS control method numerically.

The obtained results are important clues to develop a new control method for carrying the vehicle along the LIM guide way. Moreover, the theoretical approach of the stability and the onset of chaotic motion by the VSS control method is inevitable.

Acknowledgement

The authors would like to acknowledge the contributions of Mr. M. Yanagita, Mr. T. Hirata and Mr. H. Fukakusa, who are former students, for their effort to develop the system and to analyze it.

References

[1] T. Hikihara, T. Hirata and Y. Hirane, A magnetic suspension system of linear induction motor – Control method and stability of suspended motion, Proc. 11th Int. Conf. on Maglev, Maglev' 89, July 1989, p. 203–208.

[2] T. Hikihara, T. Hirata, T. Kitai and Y. Hirane, Levitation control of a magnetic suspension system of linear induction motor, Proc. IEEE Int. Workshop on Advanced Motion Control, Yokohama, March 1990.
[3] T. Hirata, T. Hikihara and Y. Hirane, Suspension characteristics of magnetic suspension system by linear induction motor, Trans. IEE Japan 110D (1990) 1091 (in Japanese).
[4] V.I. Utkin, Variable structure systems with sliding modes, IEEE Trans. AC-22 (1977) 212.
[5] F.C. Moon, Chaotic Vibrations (Wiley-Interscience, New York, 1987).
[6] J. Guckenheimer and P. Holmes, Nonlinear Oscillations, Dynamical Systems, and Bifurcations of Vector Fields (Springer, Berlin, 1986).
[7] J.M.T. Thompson and H.B. Stewart, Nonlinear Dynamics and Chaos (Wiley, New York, 1986).
[8] T. Uehara, N. Inaba and S. Mori, Chaotic phenomena in an auto gain controlled oscillator using a pulse width controller, Trans. IEICE Japan J72-A (1989) 760 (in Japanese).